Integrated kinetics-computational fluid dynamic-optimization for catalytic hydrogenation of CO_2 to formic acid

Tesfalem Aregawi Atsbha [a,1], Taeksang Yoon [b,1], Ali Cherif [b,g], Arash Esmaeili [b], Mohamed Atwair [a,h], Kwangho Park [c], Changsoo Kim [c], Ung Lee [c,d,e], Sungho Yoon [f], Chul-Jin Lee [a,b,*]

[a] Department of Intelligent Energy and Industry, Chung-Ang University, 84 Heukseok-ro, Dongjak-gu, Seoul, Republic of Korea
[b] School of Chemical Engineering and Materials Science, Chung-Ang University, 84 Heukseok-ro, Dongjak-gu, Seoul, Republic of Korea
[c] Clean Energy Research Center, Korea Institute of Science and Technology, Hwarang-ro 14–5 Seongbuk-gu, Seoul 02792, Republic of Korea
[d] Division of Energy and Environmental Technology, KIST School, Korea University of Science and Technology (UST), Seoul 02792, Republic of Korea
[e] Green School, Korea University, Anam-ro 145, Seongbuk-gu, Seoul 02841, Republic of Korea
[f] Department of Chemistry, Chung-Ang University, 84 Heukseok-ro, Dongjak-gu, Seoul, Republic of Korea
[g] Bureau of Economic Geology, The University of Texas at Austin, Austin, TX 78758, USA
[h] Department of Chemical Engineering, University of South Carolina, Columbia, South Carolina 29208, USA

ARTICLE INFO

ABSTRACT

As enormous research findings indicate, carbon dioxide (CO_2) can be converted to important products such as formic acid using catalytic hydrogenation of CO_2 technologies. In this work a three-dimensional computational fluid dynamic (CFD) reactor model for the catalytic hydrogenation of CO_2 to formic acid in the presence of triethylamine and water was developed, and the nature of the flow and reaction occurring inside the reactor was demonstrated. A kinetic model which estimates kinetic rate expressions was also developed and validated using experimental data. The kinetic parameters from the kinetic model were used as reaction source terms for the CFD reactor model development. Sensitivity analyses were performed on the design variables by integrating the kinetic parameters from the developed kinetic model. The Bayesian optimization algorithm was used to optimize the catalytic CO_2 hydrogenation reactor. The optimal design was acquired, and the CO_2 conversion increased by 32.6% compared to the initial base case. An optimized reactor design was proposed for the catalytic hydrogenation of CO_2 to formic acid within a catalytic trickle-bed reactor based on the integration of reaction kinetic modeling and CFD analysis. The integrated kinetic-CFD-optimization framework proposed in this work was effectively applied to the catalytic CO_2 hydrogenation reactor and the results reported on this work could give important design and operational insight to the further development of catalytic CO_2 hydrogenation reactors for CO_2 to formic acid conversion in carbon capture and utilization applications.

1. Introduction

Carbon dioxide (CO_2), a well-known greenhouse gas that is essential for regulating the Earth's temperature, plays a significant role in the Earth's climate system. It acts like a blanket around the globe, trapping heat and radiation coming from the sun and blocking it from going back into space. It is a naturally occurring gas that is released into the atmosphere through natural processes such as volcanic activity. However, human actions such as the use of fossil fuels, deforestation, and industrial processes significantly boosted the concentration of CO_2 in the environment, leading to an enhanced greenhouse effect and prompting global warming. As the Intergovernmental Panel on Climate Change (IPCC) report indicates, CO_2 is the most significant long-lived greenhouse gas in the environment, accounting for approximately 75% of the total warming effect caused by human activities. The rise in CO_2 concentrations mainly starting from the industrial revolution has been produced by human activities such as the use of fossil fuels and deforestation. This has led to an enhanced greenhouse impact, triggering global warming, rising sea levels, and other impacts on the planet's climate system. [1–3].

CO_2 is a major contributor to climate change, but it also presents an

---

Nomenclature

u	Velocity in the x-direction, (m/s).	D_i	Diffusion coefficient for each species (m²/s).
v	Velocity in the y-direction (m/s).	A_o	Pre-exponential factor.
w	Velocity in the z-direction (m/s).	α	Rate exponent of H_2.
q_i	Energy source or sink.	β	Rate exponent of CO_2.
S_i	Viscous and inertial losses encountered in the porous catalytic region.	R	Gas constant (8.314 J·K^{-1}·mol^{-1}).
ε	Porosity.	ρ_b	Bulk density of the catalyst.
Cp	Heat capacity (Jmol^{-1} K^{-1}).	Z	catalyst bed length.
K	Thermal conductivity.	$r_{i,j}$	ith reaction for component j.
T	Temperature.	u_s	Fluid velocity.
ρ	Density in kg/m³.	C	Concentration.
ρ_f	Density of fluid.	kg$_{cat.}$	Kilogram of catalyst.
ρ_s	Density of solid.	SST	Total sum of squares.
E_a	Activation energy.	SSR	Residual sum of squares.
R_i	Rate of each species production because of the chemical reactions.	$y_{exp,i}$	Experimental value.
		$\overline{y_{exp}}$	Average of experimental value.
		$y_{calc,i}$	Calculated value.
n_i	Species molar fraction.	TREA	Triethylamine.

opportunity to produce valuable chemicals through different methods of carbon dioxide utilization. The utilization of CO_2 as a raw material for the synthesis of chemicals has gained significant interest in recent years because of its potential to mitigate climate change and provide a sustainable source of carbon. Researchers have been exploring various methods to transform CO_2 into valuable products such as fuels, plastics, and building materials [4–9]. CO_2 has been used to synthesize chemicals, such as soda Solvay, salicylic acid, and urea, since the early days of the chemical industry. The current rise in oil prices and the new understanding of the need to lower the climate change impact of the overall chemical and energy industry, and particularly the emission of CO_2, has incited a renewed attention in matters for instance, the use of renewable resources of energy and substitute feedstock for the chemical industry, two topics that one way or another merge into the enhanced industrial utilization of CO_2 [10,11]. CO_2 utilization, one of the major focus research areas in relation to environmental and energy concerns, is gaining higher attention in the scientific community and industrial firms to change from conventional fossil-based processes toward environmentally sustainable processes. Carbon capture and utilization (CCU) technology has been considered as one of the most encouraging technologies to deal with such challenges [12].

Catalytic hydrogenation of CO_2 which is one of the essential pathways used in CCU, transforms CO_2 into energy products such as formic acid. Therefore, enormous quantities of CO_2 can be recycled through the catalytic hydrogenation of CO_2 [13,14]. Catalytic CO_2 hydrogenation is one CCU technology with the greatest possibility of being commercialized on a large scale. There are many possible catalytic CO_2 hydrogenation pathways, including those that produce formic acid, methanol, dimethyl ether (DME), and methane [15–18].

It is believed that using CO_2 as a platform molecule to produce formic acid via catalytic conversion is both an encouraging approach for effective hydrogen storage practices and an optional approach for CO_2 storage [19,20]. Formic acid, found because of CO_2 hydrogenation, has currently drawn significant interest from the scientific community and industrial firms as a chemical hydrogen (H_2) storage medium. Formic acid appears as liquid phase at ambient conditions. As a result, there is no requirement to store it under high-pressure or utilizing cooling in pricey storage unlike methane, hydrogen, and ammonia [21,22]. Formic acid obtained from CO_2 is a suitable option for hydrogen storage since it is capable of offering 4.4 wt% of hydrogen with superior atom efficiency and less toxicity. Formic acid has gained increasing attention as a favorable hydrogen storage material due to its high hydrogen content and ease of storage and transport. Moreover, it can release hydrogen at

mild conditions and with the aid of catalysts [23]. The conversion of formic acid to hydrogen is a relatively straightforward process, which can be performed on demand, making it a suitable option for stationary and mobile applications [24]. Therefore, formic acid is a promising alternative to traditional hydrogen storage methods and has the potential to contribute significantly to the development of clean energy technologies.

Additionally, formic acid can be used in various industries, such as the textile, pharmaceutical, and food chemical industries, because of its strong acidic nature and reducing properties [25,26]. Formic acid is mainly used as animal feed, a silage additive, and a preservative, which account for about 34%, 19%, and 15% of the global demand, respectively [27].

In spite of the large quantity of CO_2 availability, the primary obstacle towards catalytic conversion of CO_2 is related with its inert behavior of this molecule. Even though formic acid is capable of acquiring high hydrogen density, and thus is believed to be best for storage of energy, its manufacture from CO_2 and H_2 endures unfavorable thermodynamic conditions. Thus, the essential work focuses on developing active, selective, and stable catalysts as well as gaining an appropriate knowledge of the reactivity of CO_2 in various catalytic reaction conditions [28,29]. The most effective homogeneous catalysts for CO_2 catalytic hydrogenation to formic acid have been discovered to be complexes of metals from groups 8–10, commonly with halides or hydride as phosphines and anionic ligands as neutral ligands [30]. Homogeneous catalysts have demonstrated outstanding performance for the CO_2 catalytic conversion to formic acid in various research activities [31–35]. However, the challenges in the recovery of the catalyst from formic acid moved the research focus toward heterogeneous catalysts [36–38].

The advancement of heterogeneous catalysts for catalytic hydrogenation of CO_2 to formic acid is obtaining high attention [39]. Important advantages of the heterogeneous catalysts over homogenous catalysts for catalytic hydrogenation of CO_2 to formic acid are the relatively easy recovery of the catalyst from the respective mixed product in the downstream process, along with the stability and reusability of the catalyst [40–42].

Gunasekar et al. (2019) conducted experiment on heterogenous Ru complex catalyst supported on a bipyridyl-functionalized covalent triazine framework [bpyCTF-RuCl₃], for the conversion of CO_2 to formate and turnover frequency as high as 38800 per hour were reported.

B. Chen et al. (2020) investigated polymer-coordinated mononuclear heterogeneous Ru catalysts (Ru/p-dop-POMs) and exhibited good

catalytic activity (TON up to 25400).

In this study, a pilot scale experiment with a formic acid production capacity of ten kilograms per day was conducted to acquire kinetic data using Ru/TN-CTF catalysts. Using the pilot scale experimental data, a novel kinetic model and three-dimensional CFD reactor model was developed. Optimization framework was developed and applied for optimizing the CO_2 catalytic hydrogenation reactor to upgrade the CO_2 conversion and as a result maximizing the formic acid productivity in industrial level application.

The novel aspects of this work are summarized as follows:

(i) A three-dimensional CFD reactor model was developed, and the nature of the flow and reaction occurring inside the reactor was demonstrated.

(ii) Kinetic model was developed to integrate reaction source terms for the CFD reactor modelling. The kinetic model used in this work for the catalytic hydrogenation of CO_2 to formic acid was developed and validated using experimental data. Sensitivity analyses were also performed on the design variables by integrating the kinetic parameters from the developed kinetic model with the three-dimensional CFD reactor model.

(iii) The Bayesian optimization algorithm was used to optimize the catalytic CO_2 hydrogenation reactor. Through integration of reaction kinetic modelling and CFD analysis study we have suggested optimized reactor design for CO_2 catalytic hydrogenation to formic acid process within a catalytic trickle bed reactor.

(iv) The integrated kinetic-CFD-optimization framework proposed in this work was effectively applied to the catalytic CO_2 hydrogenation reactor.

This paper contains three main sections. The first section discusses the development and validation of the kinetic model using experimental
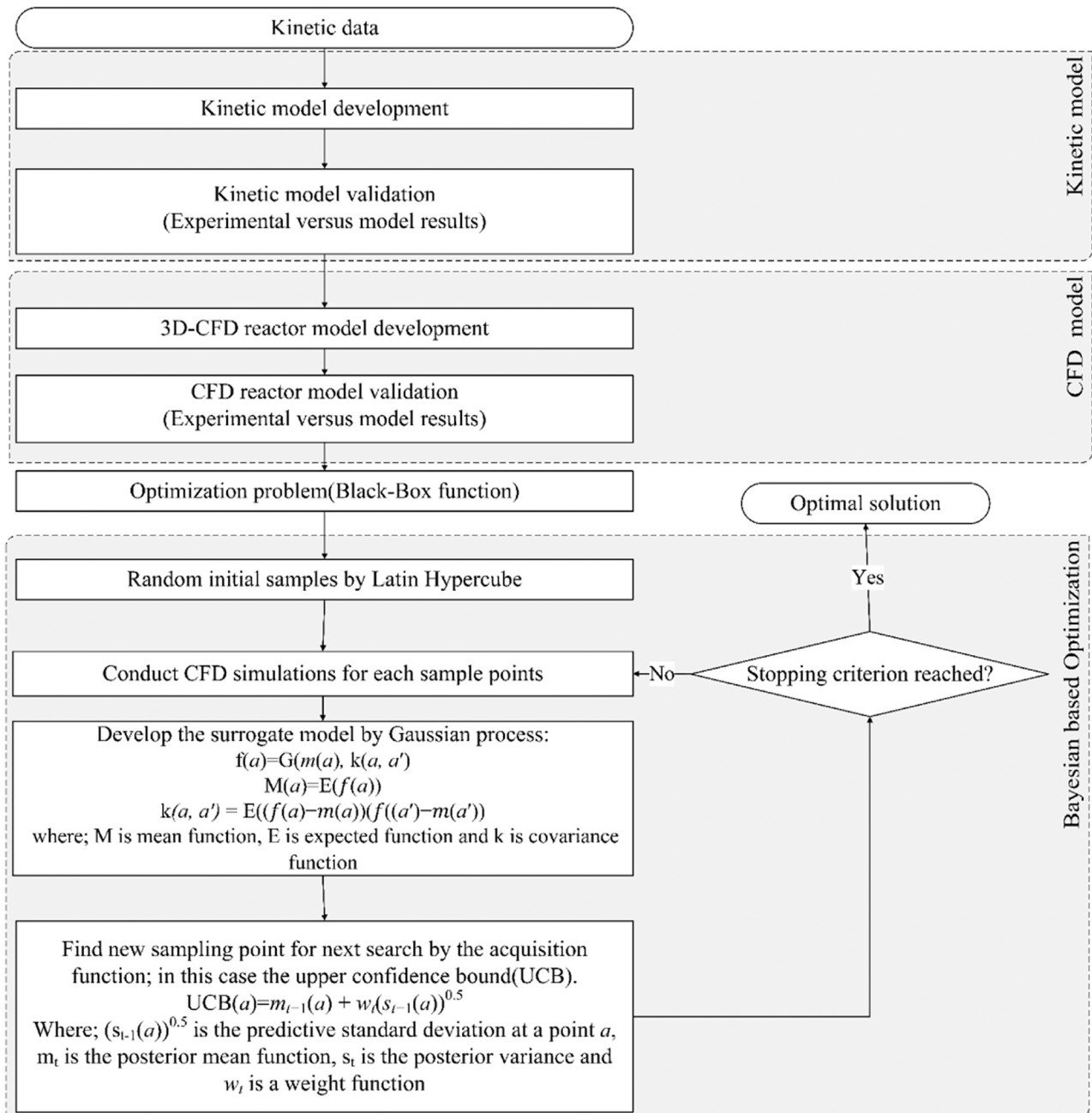

Fig. 1. Integrated kinetic-CFD-optimization framework proposed in this work.

data. The validation was achieved using actual experimental results to assure the reliability of model results. In the second part the kinetic model parameters were used to develop the CFD reactor model. The third section discusses the Optimization framework development using the Bayesian optimization algorithm and optimization of the catalytic CO_2 hydrogenation reactor. Fig. 1 shows the integrated kinetic-CFD-optimization framework developed in this work.

2. Methods

2.1. Experimental and kinetic model development

2.1.1. Experiment

Triethylamine (99%) and Ruthenium (III) chloride hydrate were purchased from Sigma-Aldrich Co. CO_2, H_2 and N_2 were acquired from Sinyang Gas Industries. Ru/TN-CTF catalyst employed for the catalytic system was prepared according to the previous study [25].

High-performance liquid chromatography (HPLC) was performed to determine the formic acid molar concentration using a YL 9100 Plus HPLC system (YL Instruments Co. Ltd., Korea) with a refractive index detector and an Aminex HPX-87 H column. The column was operated at 50 °C, and an eluent (5 mM H_2SO_4 solution) was used at a flow rate of 0.6 mL min^{-1}.

The catalytic system for the conversion of CO_2 to formic acid was validated using a trickle-bed reactor with an inner diameter of 4.8 cm, a height of 47 cm, and a production scale of 10 kg formic acid per day. First, 100 g of the powdered Ru/TN-CTF catalyst (Ru content: 0.748 wt %) meshed with 250 μm was loaded in the center of the tube reactor with a catalyst bed elevation of 10 cm, and the void space filled with glass wools and beads. During the experiment, pressure drop was negligible. A series of reactions were performed under varied reaction parameters such as temperature, pressure, and liquid feed flow. The desired reaction temperature and pressure were monitored using an electric furnace and a back-pressure regulator, respectively. The hydrogen gas feed flow was monitored by a mass flow controller, and the liquid CO_2 feed supplied from a high-pressure reservoir was regulated by a high-pressure liquid pump. The liquid feed flow rates of water and triethylamine were separately controlled using a high-pressure liquid pump.

The gas and liquid feed were well mixed and heated to the design temperature through tubular preheating zone with an inner diameter of 4.8 cm and height of 47 cm. CO_2 was well absorbed inside the reactor due to the high pressure of CO_2 and the packing of glass beads in the pre-heater. This resulted in the presence of a triethylamine-bicarbonate solution after passing through the pre-heater. For each experimental condition, a stabilization period of one hour were allowed before taking samples for testing. To confirm the reactor has stabilized under the given conditions, the reactor was analyzed its activity at regular intervals over three separate instances. The measured samples exhibited consistent and stable behavior, indicating that each condition was stabilized. The liquid samples were collected at 1 h intervals for 3 h after the temperature of reactor was stabilized to the desired point. After the operation, HPLC was used to determine the formic acid concentration under the desired reaction condition by averaging the molar concentration of formic acid obtained from liquid. Fig. 2 shows the schematic view of the trickle bed reactor system used in the experiment in this investigation to obtain the kinetic data.

2.1.2. Kinetic model development

This work focuses on the synthesis of formic acid from H_2 and CO_2 using Ru/TN-CTF catalysts with pressure from 80 bar to 120 bar and temperatures from 80 °C to 120 °C in accordance with the general equation shown in Eq. 1:

$$CO_2 + H_2 \xrightarrow[\text{H}_2\text{O}]{\text{Base(TREA)}} HCOOH \tag{1}$$

The kinetic model was developed based on the power law described in Eq. 3. Catalyst deactivation is assumed to be neglected. The vapor-
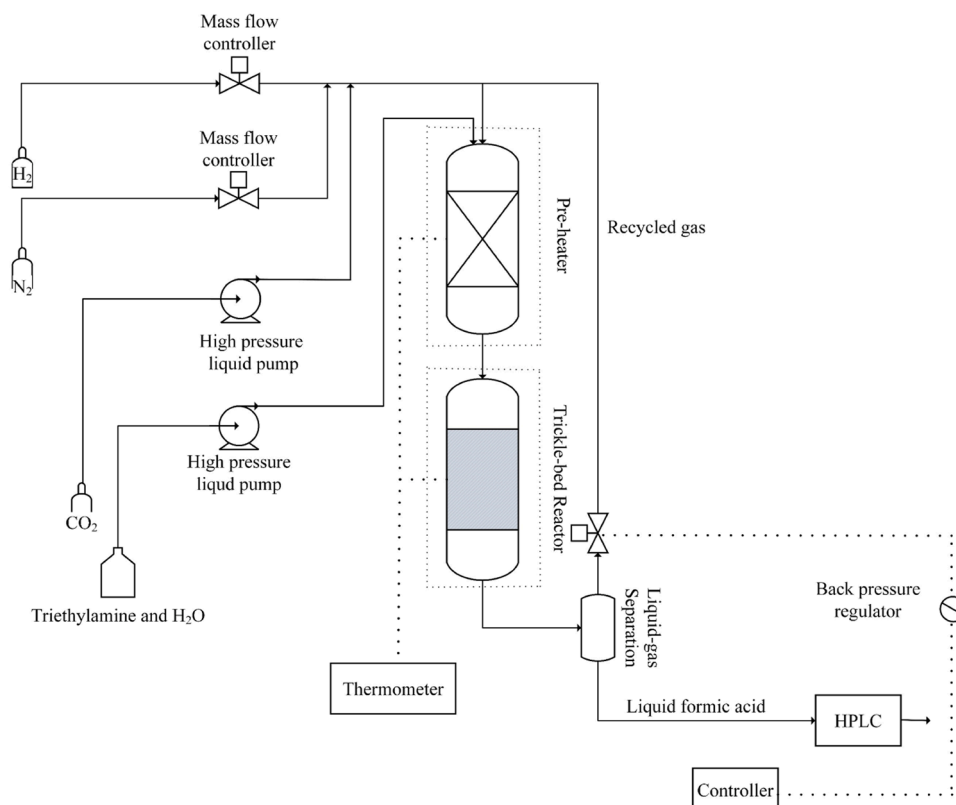

Fig. 2. Flow scheme of the equipment used for acquiring the kinetic data.

liquid equilibrium state of gas component in the solution was expressed as follows with Henry's law [43]:

$$k_{h,g}(T) = k_{h,g}(298.15) * \exp\left(\frac{d(\ln(k_H))}{d(1/T)}\right) \qquad (2)$$

$k_{h,g}(T)$ is Henry constant at temperature T of gas g. The molar amount of gas in liquid was reflected as follows.

$$n_g(T) = k_{h,g}(T) * P_g * m_{H2O} \qquad (3)$$

P_g is partial pressure of gas g and m_{H2O} is mass amount of water in feed. The concentration of hydrogen was reflected as the saturation concentration of hydrogen in the solution. The Henry constant of hydrogen was applied to calculate the saturation concentration. The developed power law-based kinetic model was preferred in this work due to its compatibility with CFD reactor model development. This implies that the kinetic parameters can be directly incorporated in to the CFD reactor model in the simulator.

$$r = kC_{H2}^{\alpha}C_{CO2}^{\beta} \qquad (4)$$

where the reaction rate constant k can be stated as a function of temperature using the Arrhenius equation:

$$k = A\exp\left(-\frac{E_a}{RT}\right) \qquad (5)$$

Additionally, the relationship between the CO_2 concentration and the formic acid production rate was discovered to be zero order reaction in earlier research; therefore, the order of CO_2, β, was assumed as zero, and the equation was simplified as follows [44]:

$$r_i = A\exp\left(-\frac{E_a}{RT}\right)C_{H2}^{\alpha} \qquad (6)$$

To ascertain the presence of mass transfer limitation during the reaction, Mears parameter of the reaction was calculated. The Mears parameter value in this experiment was less than 0.15, indicating negligible external mass transfer diffusion. Therefore, the following mass balance equation was used for the plug flow model:

$$\frac{dC}{dZ} = \frac{\rho_b}{u_s}\sum_{j=1}^{N} r_{i,j} \qquad (7)$$

The precision of kinetic parameters was confirmed based on the coefficient of determination (R^2), which can be expressed as follows:

$$R^2 = 1 - \frac{SSR}{SST} \qquad (8)$$

$$SST = \sum_{i=1}^{n}\left(y_{exp,i} - \overline{y_{exp}}\right)^2 \qquad (9)$$

$$SSR = \sum_{i=1}^{n}\left(y_{exp,i} - y_{calc,i}\right)^2 \qquad (10)$$

2.2. CFD model development

Three-dimensional CFD simulations were conducted using a reactive porous medium model. The software package ANSYS FLUENT 19.1 was used as the computational code. The catalytic zone was the focus of the computational domain. The feed components were assumed to be mixed as well as heated before entering the reactor and entering at a steady flow condition through the inlet of the porous catalytic zone. The trickle bed reactor packed with catalyst particles was assumed to be a continuous porous medium.

Porous zone of trickle bed reactor was considered between inlet and outlet of fluid and boundary condition was considered between porous in and porous out. As a result, three-dimensional cylindrical geometry was designed with the same dimensions as the catalytic bed used in the experiment (4.8 cm diameter and 10 cm height). Three-dimensional mesh was constructed based on the catalytic bed section of the reactor geometry and computational domain was generated. The generated mesh consists tetrahedral elements of 0.005 m in size, resulting in a total of 26,438 elements and 63,189 nodes using patch conforming algorithm for the base case (see supplementary Fig. S2). In addition, a mesh independency study was also conducted to observe the effect of grid size on the numerical accuracy and computational time.

To investigate mesh independence, sensitivity analysis with three different mesh sizes namely the course mesh (13,274 elements), medium mesh (26,438 elements) and fine mesh (79,576 elements) were conducted. The mass fraction on the particle surfaces indicated slight deviation between the different investigated meshes (see supplementary Fig. S3 and S4). However, there were no deviations observed between the medium and fine mesh. As can be seen from Table 1, the mesh size with 0.005 m is used considering the lower computational time compared to the fine mesh. The reactor walls were assumed as no-slip boundary conditions. The catalytic loading was estimated based on the Ru based catalyst (Ru/TN-CTF) surface-to volume ratio obtained from the experimental value. Accordingly, it was computed to be 2.19×10^9 m^{-1} (total pore volume 0.57 cm^3 g^{-1}, surface area 1251 m^2 g^{-1}).

Using semi-empirical Ergun equation, a flow resistance was employed to the porous catalytic area which refers for the viscous and inertial losses encountered through the porous media [45]. Catalyst particles with particle size 2.50×10^{-4} m and bulk porosity(ε) of 0.538 were used to compute the inertial and viscous losses experienced through the porous media.

$$\left(\frac{1}{\beta}\right) = \frac{150(1-\varepsilon)}{D_p^2\varepsilon^3} \qquad (11)$$

$$C_2 = \frac{3.5(1-\varepsilon)}{D_p\varepsilon^3} \qquad (12)$$

Where, C_2 is inertial resistance, $(1/\beta)$ is viscous resistance, D_p is average particle diameter or pore size in porous media. Table 2 shows properties of porous media used for modeling. The SIMPLE algorithm was applied for pressure and velocity coupling with second-order upwind method for spatial discretization of momentum, species, as well as energy equations.

CO_2 conversion was calculated using the following equation:

$$\text{Conversion}(x) = \frac{(CO_{2in} - CO_{2out})}{CO_{2in}} \times 100 \qquad (13)$$

The governing equations used in this study are expressed as follows: The continuity equation:

$$\left(\frac{\partial\rho u}{\partial x} + \frac{\partial\rho v}{\partial y} + \frac{\partial\rho w}{\partial z}\right) = 0 \qquad (14)$$

Momentum equations:

$$\rho\left(u\frac{\partial u}{\partial x} + v\frac{\partial u}{\partial y} + w\frac{\partial u}{\partial z}\right) = -\frac{\partial p}{\partial x} + \frac{\partial}{\partial x}\left(\mu\frac{\partial u}{\partial x}\right) + \frac{\partial}{\partial y}\left(\mu\frac{\partial u}{\partial y}\right) + \frac{\partial}{\partial z}\left(\mu\frac{\partial u}{\partial z}\right) + S_i \qquad (15)$$

Table 1
Grid independence study results with various mesh sizes.

Mesh size (m)	Number of total elements	Number of total nodes	Average time per iteration (seconds)	CO2 conversion
0.003	79,576	183,142	0.093	41.3
0.005	26,438	63,189	0.034	41.3
0.007	13,274	32,741	0.018	41.2

Table 2
Properties of porous media in the reactor.

Parameters	Values
Porosity (ε)	0.538
Inertial loss (m^{-1})	8.3×10^6
Viscous resistance (m^{-2})	1.32×10^{14}

$$\rho\left(u\frac{\partial v}{\partial x} + v\frac{\partial v}{\partial y} + w\frac{\partial v}{\partial z}\right) = -\frac{\partial p}{\partial y} + \frac{\partial}{\partial x}(\mu\frac{\partial v}{\partial x}) + \frac{\partial}{\partial y}(\mu\frac{\partial v}{\partial y}) + \frac{\partial}{\partial z}(\mu\frac{\partial v}{\partial z}) + S_i$$

$$\rho\left(u\frac{\partial w}{\partial x} + v\frac{\partial w}{\partial y} + w\frac{\partial w}{\partial z}\right) = -\frac{\partial p}{\partial z} + \frac{\partial}{\partial x}(\mu\frac{\partial w}{\partial x}) + \frac{\partial}{\partial y}(\mu\frac{\partial w}{\partial y}) + \frac{\partial}{\partial z}(\mu\frac{\partial w}{\partial z}) + S_i$$

Energy equations:

$$\rho Cp\left(u\frac{\partial T}{\partial x} + v\frac{\partial T}{\partial y} + w\frac{\partial T}{\partial z}\right) = \frac{\partial}{\partial x}\left(k\frac{\partial T}{\partial x}\right) + \frac{\partial}{\partial y}\left(k\frac{\partial T}{\partial y}\right) + \frac{\partial}{\partial z}\left(k\frac{\partial T}{\partial z}\right) + q_i$$

(16)

$$\rho = \rho f + (1 - \varepsilon)\rho s \tag{17}$$

Species transport:

$$\left(u\frac{\partial\rho n_i}{\partial x} + v\frac{\partial\rho n_i}{\partial y} + w\frac{\partial\rho n_i}{\partial z}\right) = \frac{\partial}{\partial x}\left(D_i\frac{\partial\rho n_i}{\partial x}\right) + \frac{\partial}{\partial y}\left(D_i\frac{\partial\rho n_i}{\partial y}\right) + \frac{\partial}{\partial z}\left(D_i\frac{\partial\rho n_i}{\partial z}\right) + r_i$$

(18)

2.3. Bayesian optimization

The operating conditions with respect to which the objective function could be optimized are inlet temperature, inlet mass flowrate, wall temperature and triethylamine concentration (water triethylamine molar ratio). Combining optimization algorithm with sensitivity analysis facilitates an effective optimization. Screening the input variables by applying sensitivity analysis facilitates optimization with a speedy-converging practice by reducing the size of the search space [46]. As can be observed from Fig. 3, the effect of sensitivity analysis indicated that the effect of inlet temperature and inlet mass flowrate were not significant on formic acid productivity compared to the wall temperature. As a result, inlet temperature and inlet mass flow rate were kept constant. The effect of triethylamine concentration also doesn't seem to highly affect the formic acid productivity compared the wall
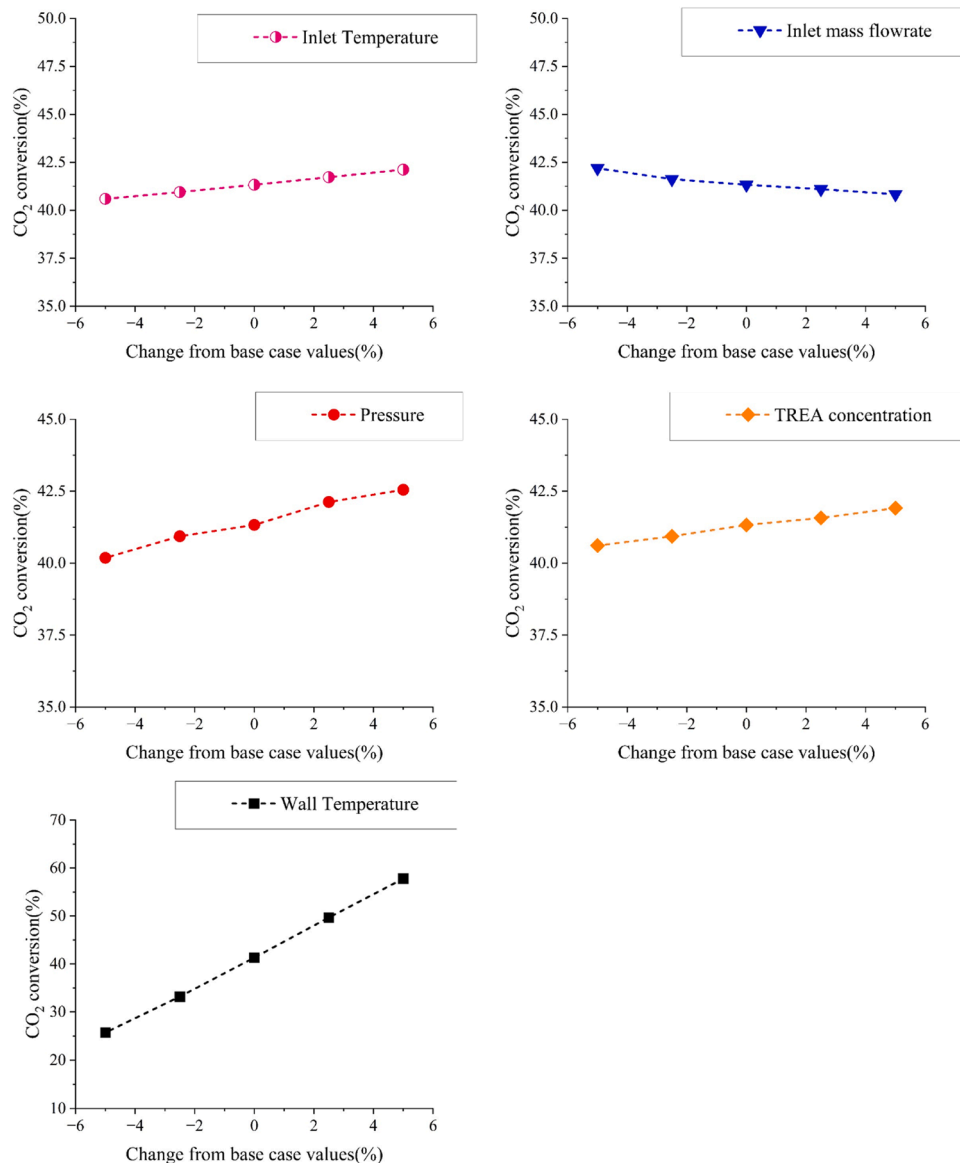

Fig. 3. Sensitivity analysis results of various design variables.

temperature. However, in energy point of view, the higher amount of water content demands elevated energy use in the downstream separation process to separate formic acid [25]. Hence, wall temperature, operating pressure, and triethylamine concentration is adopted for the design variable in Bayesian optimization.

Bayesian optimization is an optimization methodology (algorithm) for optimizing objective functions that take a long time to assess. It is generally used for expensive, unknown, or derivative-free objective functions. It develops a surrogate model for the objective function and measures the uncertainty in that surrogate using Gaussian process regression, and then utilizes an acquisition function specified from this surrogate to determine where to sample. Mathematically describing, Bayesian optimization is designed for finding global maximum or minimum of an expensive or black-box function f(a), under the condition where f(a) obtains an input amount or quantity a [47].

In the CO_2 catalytic hydrogenation reactor design, the objective function of formic acid formation with the design parameters does not provide function derivatives, so its derivative couldn't be identified. Numerous optimization algorithms can be used for black-box functions optimization, for instance evolutionary algorithms such as genetic algorithm. However, these optimization algorithms are not as sample efficient as Bayesian optimization due to the need of many function assessments to execute optimization[48]. Bayesian optimization uses a model-based method with an adaptive sampling strategy to reduce the number of function assessments. Therefore, the Bayesian optimization algorithm was implemented for CO_2 catalytic hydrogenation reactor optimization. On this research a indicates the design variables used, namely the wall temperature, pressure, and triethylamine concentration, and f(a) was the CO_2 conversion which was evaluated using the CFD model.

Bayesian optimization combines two key concepts: Gaussian process (GP) and acquisition function. A Gaussian process is described as a set of random variables, any finite number of which have a combined Gaussian distribution [49,50]. In Gaussian process regression, the output function at input a can be expressed as follows (Eq. 19):

$$f(a) \sim G(m(a), k(a, a')) \tag{19}$$

where G is the Gaussian process, which is defined by a mean (m(a)) and a kernel function (k(a, a')). The mean function indicates the likely function value at input a, and the kernel function demonstrates the reliance between the function values at various input points, a and a' [51].

By utilizing the Gaussian process model, an acquisition function which endorses the input nominee (option) to be examined for the subsequent experiment was built.

3. Results

3.1. Kinetic model estimation and validation

The parameter estimation was done by using the "lsqcurvefit" subroutine in MATLAB, where the Levenberg-Marquardt method was applied. The estimation was done by using 22 experimental data in Table 3, and the results of the estimated value, confidence interval, and the standard deviation of each kinetic parameters are listed in Table 4. The confidence interval and standard deviation of each parameter are less than half of the parameter value. Furthermore, as shown in Table 5 and Fig. 4, most of the calculated conversion value were in 10% error range of the experimental values, which can be said that the kinetic model predictions are generally in reasonable agreement with the experimental data.

3.2. CFD results

The estimated kinetic parameters from Table 3 were used for the CFD reactor model development.

The base model was validated by comparing the model reactor outlet stream with the experimental data. Fig. 5 shows the base case mass fraction of species along the reactor. The base model conversion was 41.33% at inlet conditions 117.4 mol per hour (mol/h), 393 K and

Table 4
Estimated kinetic parameters.

Parameter	Value	Confidence interval (95%)	Standard deviation
A_o ((mol/kg$_{cat}$·s).(m³/ kmol)$^{(\alpha+\beta)}$)	159.03	46.00	23.47
E_a (kJ/mol)	46.00	0.486	0.248
α	1.72	0.0235	0.012

Table 3
Pilot scale kinetic data for the CO_2 to formic acid/formate reaction using the Ru/TN-CTF catalyst with 10 kg per day capacity trickle bed reactor.

Entry	Temperature (℃)	Pressure (bar)	H_2O^l (mol/h)	TREA^l (mol/h)	CO_2^l (mol/h)	H_2^m (mol/h)	CO_2 conversion (%)	Temperature difference (ΔT) in ℃
1	80	120	183.1	17.2	17.2	17.2	9.7	0
2	100	120	183.1	17.2	17.2	17.2	15.1	1.9
3	120	100	183.1	17.2	17.2	17.2	29.6	6.8
4	80	100	183.1	17.2	17.2	17.2	7.3	0.4
5	100	100	183.1	17.2	17.2	17.2	14.1	1.4
6	80	80	183.1	17.2	17.2	17.2	5.6	0.6
7	100	80	183.1	17.2	17.2	17.2	13.5	2.7
8	80	120	137.3	12.9	12.9	12.9	10.2	0
9	100	120	137.3	12.9	12.9	12.9	16.5	2.6
10	80	100	137.3	12.9	12.9	12.9	7.8	0.2
11	100	100	137.3	12.9	12.9	12.9	15	1.7
12	120	100	137.3	12.9	12.9	12.9	31.2	6.2
13	80	80	137.3	12.9	12.9	12.9	6.6	-0.3
14	100	80	137.3	12.9	12.9	12.9	14.2	2.3
15	120	80	137.3	12.9	12.9	12.9	22	4.6
16	120	120	91.6	8.6	8.6	8.6	44.4	10.8
17	80	100	91.6	8.6	8.6	8.6	12.7	-1.3
18	100	100	91.6	8.6	8.6	8.6	18	1.7
19	120	100	91.6	8.6	8.6	8.6	33.1	5.1
20	120	80	91.6	8.6	8.6	8.6	30.2	4.1
21	80	80	91.6	8.6	8.6	8.6	9.7	-1.1
22	100	80	91.6	8.6	8.6	8.6	16.3	2.1

[l] high-pressure liquid pump was used to control liquid flow rate,
[m] mass flow controller was used to control gas flow rate, ΔT is temperature difference between inlet and outlet temperature

Table 5
Estimated and experimental CO_2 conversion.

Entry	Temperature (°C)	Pressure (bar)	Experimental CO_2 conversion (%)	Estimated CO_2 conversion (%)
1	80	120	9.7	9.73
2	100	120	15.1	15.17
3	120	100	29.6	25.65
4	80	100	7.3	6.79
5	100	100	14.1	13.41
6	80	80	5.6	5.35
7	100	80	13.5	11.91
8	80	120	10.2	10.04
9	100	120	16.5	18.34
10	80	100	7.8	8.13
11	100	100	15	15.9
12	120	100	31.2	29.57
13	80	80	6.6	6.66
14	100	80	14.2	13.81
15	120	80	22	22.94
16	120	120	44.4	43.15
17	80	100	12.7	12.34
18	100	100	18	21.05
19	120	100	33.1	36.1
20	120	80	30.2	31.24
21	80	80	9.7	8.42
22	100	80	16.3	17.74
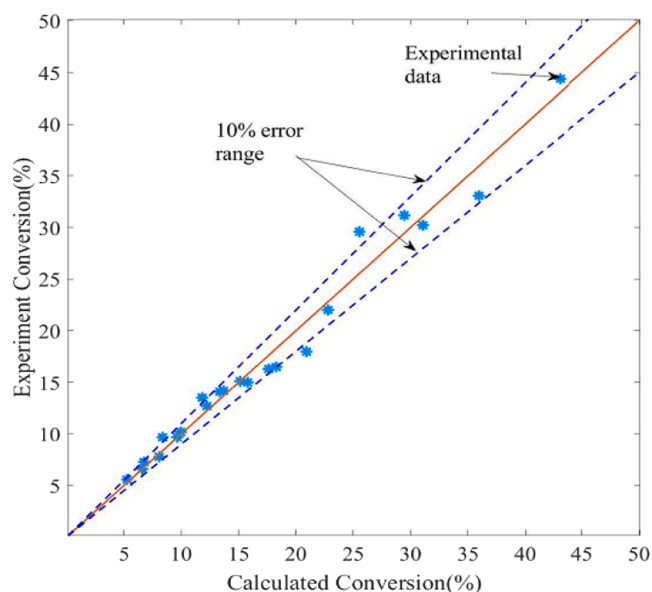
Fig. 4. Parity plots of the calculated and experimental conversion values with a 10% error range.

12 MPa. Compared to the experimental data which is 44.4%, the model appeared to underestimate. However, the error percentage is not significant (less than 10%). The outlet temperature obtained from experiment was also comparable to the simulated data obtained from the CFD analysis (simulated data outlet temperature: 405.5 K, experimental data: 403.8 K). Slight differences between experimental results and model results are expected because of the estimated parameters which are challenging to exactly determine from the experiments such as bulk porosity, inertial resistance, and viscous resistance. Understanding of the temperature profiles from the CFD as can be observed from Fig. 6 illustrates that it is likely slight overall temperature variation; though it can be stated that the availability of large proportion of water in the feed would lead to minimal temperature change. It also illustrates there was no significant local temperature variations (temperature increase) within the catalyst bed which could have adverse effects on catalyst stability or formic acid decomposition. The temperature variation

throughout the catalyst bed was not significant (not more than 1 °C) as can be seen from Fig. 6.

3.3. Optimization results

The optimization problem was set for CO_2 catalytic hydrogenation reactor by applying Bayesian optimization algorithm which is illustrated with more general form as follows:

Max $f(a)$.

Subject to: $a_i^{(L)} \le a_i \le a_i^{(U)}$, i = 1,......I,

where a indicates the design parameters, i.e., $a = [a_1, a_2, a_3]$ as a column vector and $f(a)$ was the black box function that should be optimized, in this issue the CO_2 conversion. a_1, a_2 and a_3 are the three design parameters: wall temperature, pressure, and triethylamine concentration. The lower bound for these design parameters was given as $a^{(L)}$ = [333 K, 8 MPa, 2500 mol/m^3] respectively. The upper bound for these design parameters was also given as $a^{(U)}$ = [413 K, 12 MPa, 3200 mol/m^3], respectively. The upper and lower bound values were taken according to the experimental investigation. As shown in Fig. 7 which shows the result from Bayesian optimization, the CO_2 conversion increased with number of iterations and achieved to final optimal result after total 40 function assessments. The final optimal point was achieved at the 40 assessments of the function estimation. No extra enhancement or deviation of results was observed in successive evaluations. Unlike requiring over 100 million simulations in an exhaustive grid search, the suggested optimization identified the optimal solution with just 40 function assessments. The input result at the achieved optimal point was a° = [413 K, 12 MPa, 3200 mol/m^3] and the objective function result was 58.89%, that was 32.6% increase attained from the primary base case. Fig. 8 shows mass fractions of species and localized temperature distribution along the reactor under optimal conditions. The enhancement is attributed to the improved reaction conditions. The sensitivity of the reaction to changes in temperature is related to the high activation energy (46 kJ/mol) of the reaction as reactions with high activation energy increases rapidly with increased temperature. In addition to that, the reactants solubility much increased as the pressure increased compared to the base case which enhanced the formic acid yield and CO_2 conversion.

4. Conclusion

In this study, a pilot scale experiment with a formic acid production capacity of ten kilograms per day was conducted to acquire kinetic data using Ru/TN-CTF catalysts. The integrated kinetic-CFD-optimization framework was proposed. The proposed framework was effectively applied to a practical catalytic CO_2 hydrogenation reactor. A kinetic model for the catalytic hydrogenation of CO_2 to formic acid in the form of Arrhenius equation was developed and validated using experimental data. A three-dimensional CFD reactor model was also developed, and the behavior of the flow condition and reaction taking place inside the reactor was demonstrated. Sensitivity analyses were also performed on the design variables by integrating the kinetic parameters from the developed kinetic model. The CFD reactor model was also validated by comparing it to the experimental data. The three-dimensional CFD reactor model, with the Ru-based (Ru/TN-CTF) catalyst also provides important insights on reaction rate, local temperature variations, flow situations and the component concentrations in the reactor which are vital to reactor design for optimized catalytic systems. Sensitivity analysis was conducted to identify the most sensitive design variables. The sensitivity analysis indicated wall temperature, operating pressure, and triethylamine concentration were the most sensitive design variables. Bayesian optimization algorithm was adopted for CO_2 catalytic hydrogenation reactor optimization. Through integration of reaction kinetic modelling and computational fluid dynamic analysis, optimized reactor design for CO_2 catalytic hydrogenation to formic acid process within a catalytic trickle bed reactor was suggested. The optimal design values
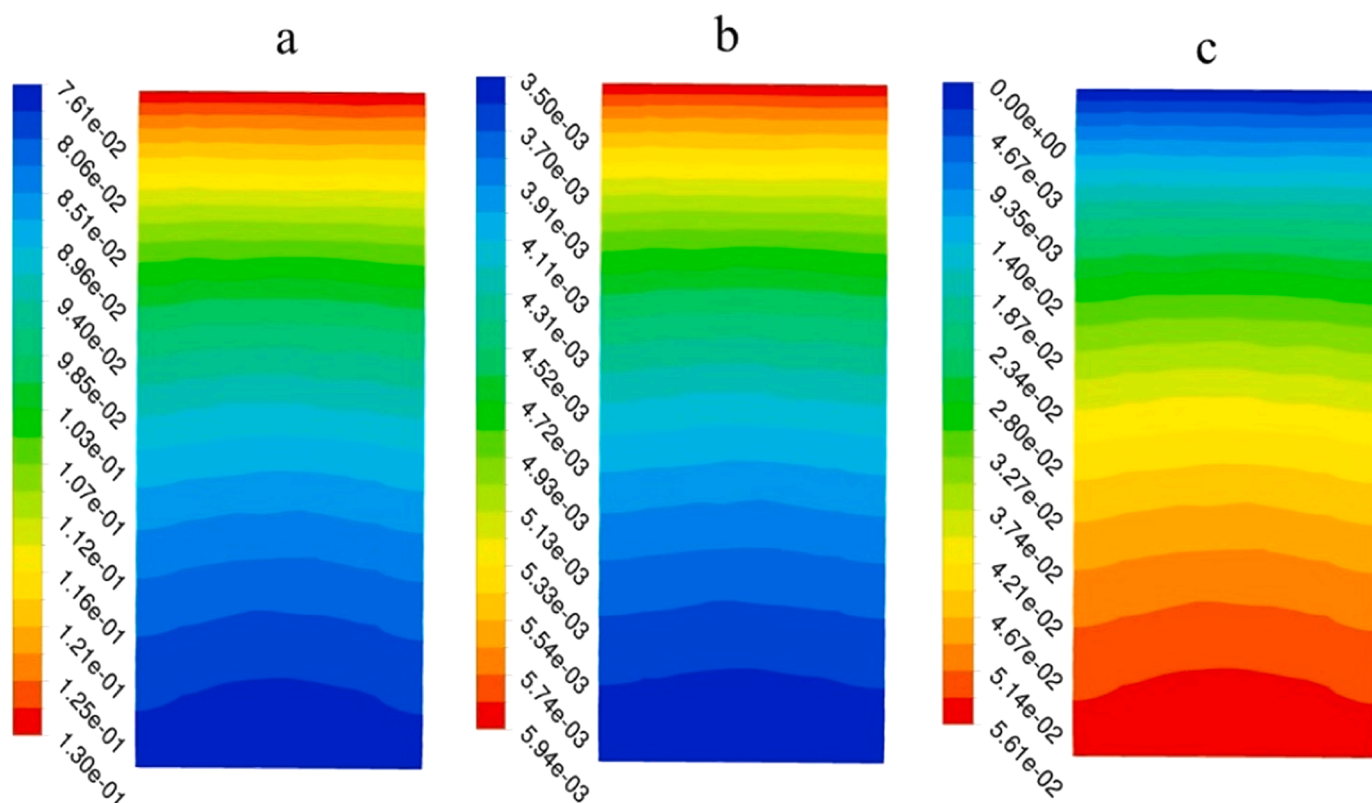
Fig. 5. Base case mass fractions of species (CO_2(a), H_2(b), and HCOOH(c)) along a two-dimensional plane surface in the center of the reactor. Inlet temperature, pressure and flowrate conditions are 393 K, 12 MPa and 117.4 mol/h, respectively.
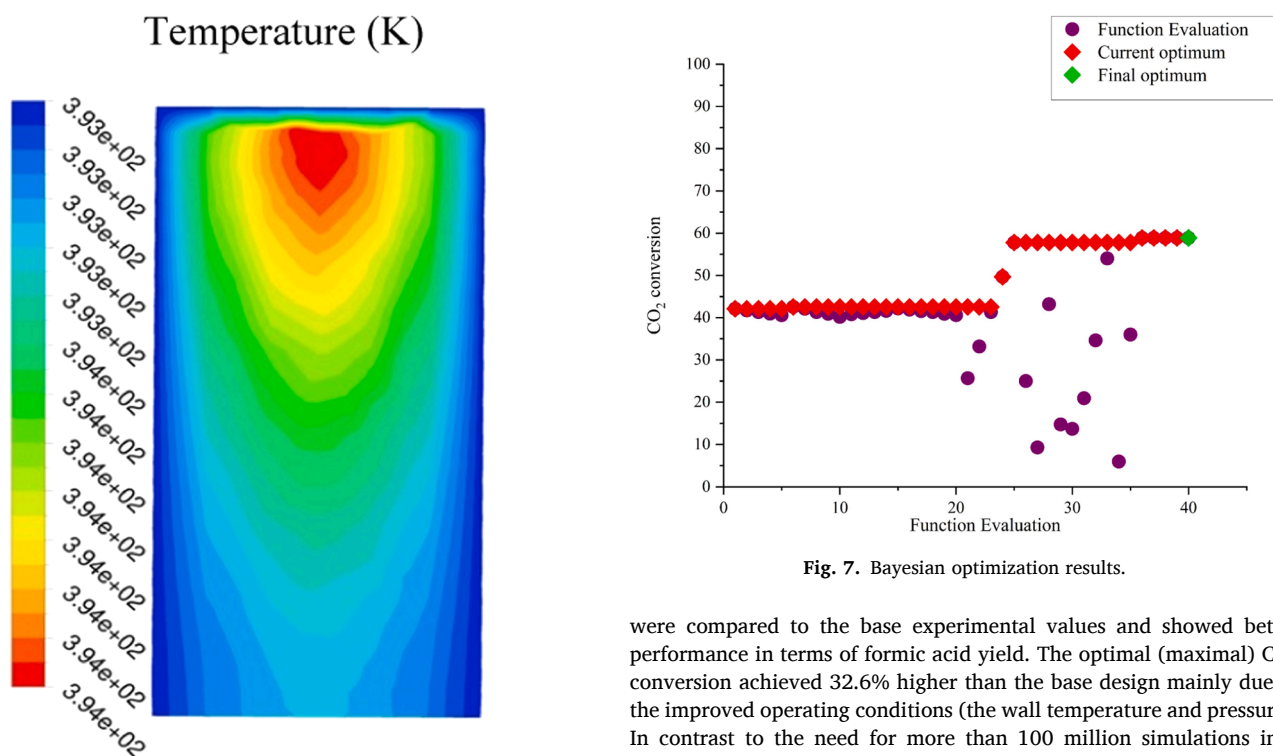

Fig. 6. Localized temperature distribution within the reactor catalyst bed along the two-dimensional plane surface at the centre of the reactor with constant wall temperature of 393 K. Inlet temperature, pressure and flowrate conditions are 393 K, 12 MPa and 117.4 mol/h respectively.

Fig. 7. Bayesian optimization results.

were compared to the base experimental values and showed better performance in terms of formic acid yield. The optimal (maximal) CO_2 conversion achieved 32.6% higher than the base design mainly due to the improved operating conditions (the wall temperature and pressure). In contrast to the need for more than 100 million simulations in a thorough grid search, only 40 function assessments were carried out to find the optimal solution using the proposed framework. This shows that the suggested approach can efficiently be applied for design and optimization of costly CFD reactor models that require a lot of computing and evaluation time. The integrated kinetic-CFD-optimization framework proposed in this work could give important design and operational
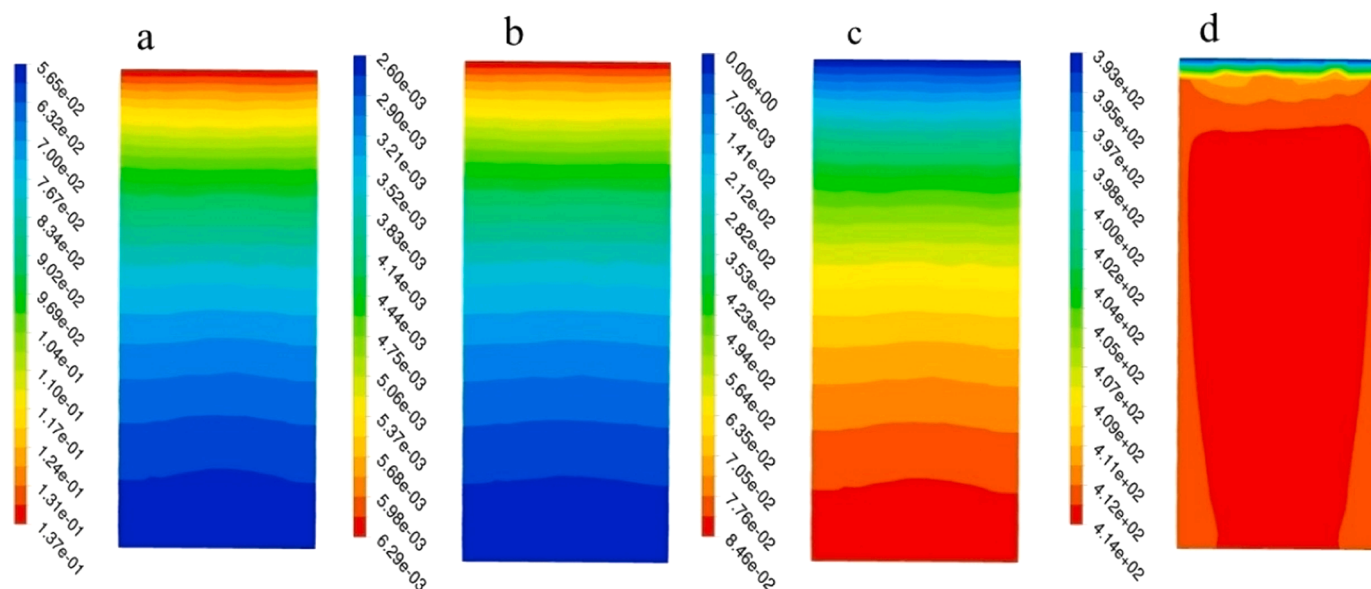
Fig. 8. Mass fractions of species(H_2(a), CO_2(b), HCOOH(c)) and temperature profile(d) along a 2D plane surface in the centre of the reactor under optimal conditions.

insight to the further development of catalytic CO_2 hydrogenation reactors for CO_2 to formic acid conversion in carbon capture and utilization applications.

CRediT authorship contribution statement

Tesfalem Aregawi Atsbha: Conceptualization, Data curation, Investigation, Methodology, Visualization, Validation, Writing - original draft, Writing - review & editing. Taeksang Yoon: Conceptualization, Data curation, Investigation, Methodology, Visualization, Validation, Writing - original draft, Writing - review & editing. Ali Cherif: Methodology, Software, Writing - review & editing. Arash Esmaeili: Methodology, Visualization, Writing - review & editing. Mohamed Atwair: Software, Methodology. Kwangho Park: Experiment, Writing - original draft. Changsoo Kim: Experiment, Writing - original draft. Ung Lee: Experiment, Writing - original draft. Sungho Yoon and Chul-Jin Lee: Funding acquisition, Project administration, Resources and Supervision.

Declaration of Competing Interest

The authors declare that they have no known competing financial interests or personal relationships that could have appeared to influence the work reported in this paper.

Data availability

Data will be made available on request.

Acknowledgments

Appendix A. Supporting information

Supplementary data associated with this article can be found in the online version at doi:10.1016/j.jcou.2023.102635.

References

[1] MD, V. *et al.* Climate change *2021*: *the physical science basis: summary for policymakers: working group I contribution to the sixth Assessment report of the Intergovernmental Panel on Climate Change.*

[2] Anne Olhoff *et al.* United Nations *Environment Programme. Emissions Gap Report 2022: The Closing Window - Climate crisis calls for rapid transformation of societies.* ⟨https://www.unep.org/emissions-gap-report-2022⟩ (2022).

[3] EPA (2023) Inventory of U.S. Greenhouse Gas Emissions and Sinks: 1990-2021.U.S. Environmental Protection Agency, EPA 430-D-23-001. http://unfccc.int (1990).

[4] S. Xie, Q. Zhang, G. Liu, Y. Wang, Photocatalytic and photoelectrocatalytic reduction of CO_2 using heterogeneous catalysts with controlled nanostructures, Chem. Commun. 52 (2016) 35–59.

[5] W. Sheng, et al., Electrochemical reduction of CO_2 to synthesis gas with controlled CO/H2 ratios, Energy Environ. Sci. 10 (2017) 1180–1185.

[6] A. Al-Mamoori, A.A. Rownaghi, F. Rezaei, Combined Capture and Utilization of CO_2 for Syngas Production over Dual-Function Materials. *ACS Sustain*, Chem. Eng. 6 (2018) 13551–13561.

[7] Izumi, Y. & oxides, Z.-C.-I. *Recent Advances (2012–2015) in the Photocatalytic Conversion of Carbon Dioxide to Fuels Using Solar Energy: Feasibilty for a New Energy .* vol. 06 ⟨https://pubs.acs.org/sharingguidelines⟩ (2023).

[8] M. Aresta, A. Dibenedetto, A. Angelini, The changing paradigm in CO_2 utilization (Preprint at), J. CO_2 Util. vols 3–4 (2013) 65–73, https://doi.org/10.1016/j.jcou.2013.08.001.

[9] C. Panzone, R. Philippe, A. Chappaz, P. Fongarland, A. Bengaouer, Power-to-Liquid catalytic CO_2 valorization into fuels and chemicals: Focus on the Fischer-Tropsch route, J. CO_2 Util. 38 (2020) 314–347.

[10] M. Aresta, A. Dibenedetto, Industrial utilization of carbon dioxide (CO_2) (Co), in: Developments and Innovation in Carbon Dioxide, vol. 2, Elsevier Ltd,, 2010, pp. 377–410 (Co).

[11] Y. Ahn, et al., System-level analysis and life cycle assessment of CO_2 and fossil-based formic acid strategies, Green. Chem. 21 (2019) 3442–3455.

[12] F. Kosaka, et al., Direct and continuous conversion of flue gas CO_2 into green fuels using dual function materials in a circulating fluidized bed system, Chem. Eng. J. 450 (2022).

[13] T.A. Atsbha, T. Yoon, P. Seongho, C.J. Lee, A review on the catalytic conversion of CO2using H2for synthesis of CO, methanol, and hydrocarbons (Preprint at), J. CO_2 Util. vol. 44 (2021), https://doi.org/10.1016/j.jcou.2020.101413.

[14] A.D.N. Kamkeng, M. Wang, J. Hu, W. Du, F. Qian, Transformation technologies for CO_2 utilisation: Current status, challenges and future prospects (Preprint at), Chem. Eng. J. vol. 409 (2021), https://doi.org/10.1016/j.cej.2020.128138.

[15] C. Ampelli, S. Perathoner, G. Centi, Co2 utilization: An enabling element to move to a resource-and energy-efficient chemical and fuel production, Philos. Trans. R. Soc. A: Math. Phys. Eng. Sci. 373 (2015).

[16] T.A. Atsbha, T. Yoon, B.H. Yoo, C.J. Lee, Techno-economic and environmental analysis for direct catalytic conversion of co2 to methanol and liquid/high-calorie-sng fuels, Catalysts 11 (2021).

[17] W. Schakel, G. Oreggioni, B. Singh, A. Strømman, A. Ramírez, Assessing the techno-environmental performance of CO_2 utilization via dry reforming of methane for the production of dimethyl ether, J. CO_2 Util. 16 (2016) 138–149.

[18] J. Nyári, M. Magdeldin, M. Larmi, M. Järvinen, A. Santasalo-Aarnio, Techno-economic barriers of an industrial-scale methanol CCU-plant, J. CO_2 Util. 39 (2020).

[19] D. Kang, J. Byun, J. Han, Evaluating the environmental impacts of formic acid production from acid production from CO_2: Catalytic hydrogenation: Vs. electrocatalytic reduction, Green. Chem. 23 (2021) 9470–9478.

[20] R. Aldaco, et al., Bringing value to the chemical industry from capture, storage and use of CO 2: A dynamic LCA of formic acid production, Sci. Total Environ. 663 (2019) 738–753.

[21] B. Thijs, J. Rongé, J.A. Martens, Matching emerging formic acid synthesis processes with application requirements†, Green. Chem. 24 (2022) 2287–2295.

[22] M.G. Rasul, M.A. Hazrat, M.A. Sattar, M.I. Jahirul, M.J. Shearer, The future of hydrogen: challenges on production, storage and applications (Preprint at), Energy Convers. Manag. vol. 272 (2022), https://doi.org/10.1016/j. enconman.2022.116326.

[23] D. Mellmann, P. Sponholz, H. Junge, M. Beller, Formic acid as a hydrogen storage material-development of homogeneous catalysts for selective hydrogen release (Preprint at), Chem. Soc. Rev. vol. 45 (2016) 3954–3988, https://doi.org/ 10.1039/c5cs00618j.

[24] J. Eppinger, K.W. Huang, Formic acid as a hydrogen energy carrier (Preprint at), ACS Energy Lett. vol. 2 (2017) 188–195, https://doi.org/10.1021/ acsenergylett.6b00574.

[25] K. Park, et al., CO_2 hydrogenation to formic acid over heterogenized ruthenium catalysts using a fixed bed reactor with separation units, Green. Chem. 22 (2020) 1639–1649.

[26] I. Dutta, et al., Formic acid to power towards low-carbon economy, Adv. Energy Mater. 12 (2022).

[27] Amir, A. & Afshar, N. CHEMICAL PROFILE: FORMIC ACID. http://chemplan.biz/ chemplan_demo/sample_reports/Formic_Acid_Profile.pdf (2014).

[28] S. De, A. Dokania, A. Ramirez, J. Gascon, Advances in the design of heterogeneous catalysts and thermocatalytic processes for CO2 utilization (Preprint at), ACS Catal. vol. 10 (2020) 14147–14185, https://doi.org/10.1021/acscatal.0c04273.

[29] X.T. Cao, D.M. Kabtamu, S. Kumar, R.S. Varma, Advances in thermo-, photo-, and electrocatalytic continuous conversion of carbon dioxide into liquid chemicals (Preprint at), ACS Sustain. Chem. Eng. vol. 10 (2022) 12906–12932, https://doi. org/10.1021/acssuschemeng.2c02491.

[30] P.G. Jessop, T. Ikariya, R. Noyori, Homogeneous hydrogenation of carbon dioxide, CHEMKAL Rev. 95 (1995) 259–272.

[31] W. Lei, Carbon dioxide as a raw material: the synthesis of formic acid and its derivatives from C02, Angew. Int. Ed. Engi 34 (1995) 2207–2221.

[32] W. Wang, S. Wang, X. Ma, J. Gong, Recent advances in catalytic hydrogenation of carbon dioxide, Chem. Soc. Rev. 40 (2011) 3703–3727.

[33] L. Wu, Q. Liu, R. Jackstell, M. Beller, Recent progress in carbon dioxide reduction using homogeneous catalysts. Carbon Dioxide and Organometallics, Springer International Publishing, 2015, pp. 279–304, https://doi.org/10.1007/3418_2015_ 109.

[34] W.H. Wang, Y. Himeda, J.T. Muckerman, G.F. Manbeck, E. Fujita, CO_2 Hydrogenation to Formate and Methanol as an Alternative to Photo- and Electrochemical CO_2 Reduction (Preprint at), Chem. Rev. vol. 115 (2015) 12936–12973, https://doi.org/10.1021/acs.chemrev.5b00197.

[35] K. Sordakis, et al., Homogeneous catalysis for sustainable hydrogen storage in formic acid and alcohols (Preprint at), Chem. Rev. vol. 118 (2018) 372–433, https://doi.org/10.1021/acs.chemrev.7b00182.

[36] G.H. Gunasekar, K.D. Jung, S. Yoon, Hydrogenation of CO 2 to Formate using a Simple, Recyclable, and Efficient Heterogeneous Catalyst, Inorg. Chem. (2019), https://doi.org/10.1021/acs.inorgchem.8b03336.

[37] A.K. Singh, S. Singh, A. Kumar, Hydrogen energy future with formic acid: A renewable chemical hydrogen storage system (Preprint at), Catal. Sci. Technol. vol. 6 (2016) 12–40, https://doi.org/10.1039/c5cy01276g.

[38] G.H. Gunasekar, K. Park, K.D. Jung, S. Yoon, Recent developments in the catalytic hydrogenation of CO_2 to formic acid/formate using heterogeneous catalysts (Preprint at), Inorg. Chem. Front. vol. 3 (2016) 882–895, https://doi.org/10.1039/ c5qi00231a.

[39] Jr., J.G. G., Kim, S. & Rhodes, W.D. Turnover frequencies in metal catalysis: Meanings, functionalities and relationships. in 320–348 (2007). doi:10.1039/9781 847553294–00320.

[40] A. Behr, K. Nowakowski, Catalytic Hydrogenation of Carbon Dioxide to Formic Acid, in: Advances in Inorganic Chemistry, vol. 66, Academic Press Inc, 2014, pp. 223–258.

[41] W. Wang, S. Wang, X. Ma, J. Gong, Recent advances in catalytic hydrogenation of carbon dioxide, Chem. Soc. Rev. 40 (2011) 3703–3727.

[42] T. Schaub, R.A. Paciello, A process for the synthesis of formic acid by CO_2 hydrogenation: thermodynamic aspects and the role of CO (Preprint at), Angew. Chem. - Int. Ed. vol. 50 (2011) 7278–7282, https://doi.org/10.1002/ anie.201101292.

[43] J. Kumełan, D. Tuma, Á.L.P.S. Kamps, G. Maurer, Solubility of the single gases carbon dioxide and hydrogen in the ionic liquid [bmpy][Tf2N], J. Chem. Eng. Data 55 (2010) 165–172.

[44] Q. Liu, et al., Direct catalytic hydrogenation of CO_2 to formate over a Schiff-base-mediated gold nanocatalyst, Nat. Commun. 8 (2017).

[45] M.E. Potter, L.M. Armstrong, R. Raja, Combining catalysis and computational fluid dynamics towards improved process design for ethanol dehydration, Catal. Sci. Technol. 8 (2018) 6163–6172.

[46] F. MacH, Reduction of optimization problem by combination of optimization algorithm and sensitivity analysis, IEEE Trans. Magn. 52 (2016).

[47] S. Park, et al., Bayesian optimization of industrial-scale toluene diisocyanate liquid-phase jet reactor with 3-D computational fluid dynamics model, J. Ind. Eng. Chem. 98 (2021) 327–339.

[48] A. Cherif, R. Nebbali, C.J. Lee, Design and multiobjective optimization of membrane steam methane reformer: a computational fluid dynamic analysis, Int J. Energy Res 46 (2022) 8700–8715.

[49] S. Greenhill, S. Rana, S. Gupta, P. Vellanki, S. Venkatesh, Bayesian optimization for adaptive experimental design: a review, IEEE Access 8 (2020) 13937–13948.

[50] Srinivas, N., Krause, A., Kakade, S.M. & Seeger, M. Gaussian Process Optimization in the Bandit Setting: No Regret and Experimental Design. (2009) doi:10.11 09/TIT.2011.2182033.

[51] Schulz, E., Speekenbrink, M. & Krause, A. A tutorial on Gaussian process regression: Modelling, exploring, and exploiting functions. doi:10.1101/095190.